Available online at www.sciencedirect.com
ScienceDirect
Journal of Computational Physics 227 (2007) 877–885
JOURNAL OF COMPUTATIONAL PHYSICS
www.elsevier.com/locate/jcp

Short Note

# On the connection between the spectral volume and the spectral difference method

Kris Van den Abeele [a,*,1], Chris Lacor [a], Z.J. Wang [b]

[a] *Vrije Universiteit Brussel, Department of Mechanical Engineering, Fluid Dynamics and Thermodynamics Research Group, Pleinlaan 2, 1050 Brussels, Belgium*
[b] *Department of Aerospace Engineering, Iowa State University, 2271 Howe Hall, Ames, IA 50011, United States*

Received 11 April 2007; received in revised form 28 August 2007; accepted 30 August 2007
Available online 14 September 2007

*Keywords:* Spectral volume method; Spectral difference method

## 1. Introduction

In the last few years, two new high-order accurate methods for unstructured grids have been developed, namely the spectral volume (SV) and the spectral difference (SD) method. Both methods are related to the well-known discontinuous Galerkin (DG) method, see for instance [1], in the sense that they also use piecewise continuous polynomials as solution approximation space. The development of the SV method was mainly reported in publications by Wang [2], Wang et al. [3–5,8], Liu et al. [6] and Sun et al. [7]. Further contributions were made by Chen [12,13], Van den Abeele et al. [14] and Van den Abeele and Lacor [15]. The development of the SD method was reported more recently in publications by Liu et al. [9] and Wang et al. [10]. In 1D, the SD method is identical to the multi-domain spectral method proposed by Kopriva [11].

The SV method is strongly related to the finite volume (FV) method. As with the FV method, the SV solution variables are averaged values over control volumes (CVs) and the residuals corresponding to these solution variables can be written as the sum of the fluxes through the CV faces. The SV method differs from the FV method in the choice of the stencils used to approximate the fluxes through these CV faces. By partitioning each cell, or spectral volume (SV), into CVs in a similar way, a unique stencil, valid for all cells in the mesh, can be obtained. This is the major advantage of the SV method over high-order accurate unstructured FV methods, where these stencils depend on the local mesh geometry. At faces between two SVs, a Riemann solver is used to compute a unique flux from the two solutions in the neighbouring SVs.

Similarly, the SD method is strongly related to the finite difference (FD) method. For both the FD and the SD method, the solution variables are pointwise values, for which the residuals can be written as a function of the flux derivatives in the solution points. With the SD method the computational domain is subdivided in

* Corresponding author. Tel.: +32 26292399; fax: +32 26292880.
*E-mail addresses:* kvdabeel@vub.ac.be (K. Van den Abeele), chris.lacor@vub.ac.be (C. Lacor), zjw@iastate.edu (Z.J. Wang).
[1] FWO Research Engineer.

0021-9991/$ - see front matter 
doi:10.1016/j.jcp.2007.08.030

cells, and in each cell, solution and flux points are placed in a similar way, to arrive at a unique stencil, independent of the local mesh geometry, for the flux derivatives in the solution points. The solutions in the different cells are again coupled through Riemann solvers.

The FV and the FD method are equivalent in 1D for a uniform mesh. In this note, it will be shown that a similar equivalence exists between the SV and the SD methods. The note is further organised as follows. In Sections 2 and 3, the SV and the SD methods for 1D are briefly reviewed. The equivalence between these methods will then be proven in Section 4. In Section 5, this equivalence will be illustrated for the linear advection equation and for Burger's equation in 1D, and finally conclusions will be drawn in Section 6.

## 2. Spectral volume method in 1D

The 1D SV method is applicable to hyperbolic conservation law systems of the following form:

$$\frac{\partial \mathbf{u}}{\partial t} + \frac{\partial \mathbf{f}(\mathbf{u})}{\partial x} = 0 \tag{1}$$

with $\mathbf{u}$ a column vector containing the conserved variables and $\mathbf{f}(\mathbf{u})$ the fluxes. The computational domain $x_l \leqslant x \leqslant x_r$ over which this conservation law is valid is divided in $N$ cells (SVs) with index $i : x_{i-\frac{1}{2}} \leqslant x \leqslant x_{i+\frac{1}{2}}$, such that $x_{\frac{1}{2}} \equiv x_l$ and $x_{N+\frac{1}{2}} \equiv x_r$. For a $(p+1)$th-order accurate scheme, these cells are then further subdivided into $p+1$ CVs, with index $j$ and boundaries $x^{\mathrm{b}}_{i,j-\frac{1}{2}}$ and $x^{\mathrm{b}}_{i,j+\frac{1}{2}}$. In Fig. 1, this partitioning into CVs is shown for second- and third-order accurate SV cells. Notice that for the third-order cell, the partitioning into CVs is not uniquely defined. This is also true for higher-order SV cells. For the third-order accurate case, the partitioning has one parameter $\alpha_3$, as illustrated in the figure. Integrating (1) over each CV and applying the Gauss theorem then yields

$$\frac{\mathrm{d}\bar{\mathbf{u}}_{i,j}}{\mathrm{d}t} = -\frac{\mathbf{f}(\mathbf{u}_{i,j+\frac{1}{2}}) - \mathbf{f}(\mathbf{u}_{i,j-\frac{1}{2}})}{x^{\mathrm{b}}_{i,j+\frac{1}{2}} - x^{\mathrm{b}}_{i,j-\frac{1}{2}}} \tag{2}$$

where the $\bar{\mathbf{u}}_{i,j}$ are the averaged conserved variables over the CVs

$$\bar{\mathbf{u}}_{i,j} = \frac{1}{x^{\mathrm{b}}_{i,j+\frac{1}{2}} - x^{\mathrm{b}}_{i,j-\frac{1}{2}}} \int_{x^{\mathrm{b}}_{i,j-\frac{1}{2}}}^{x^{\mathrm{b}}_{i,j+\frac{1}{2}}} \mathbf{u}\,\mathrm{d}x \tag{3}$$

On each cell, the solution can be approximated by a polynomial $\mathbf{U}^{\mathrm{SV}}_i(t,x)$ of degree $p$

$$\mathbf{u}_i(t,x) \approx \mathbf{U}^{\mathrm{SV}}_i(t,x) \equiv \sum_{j=1}^{p+1} \bar{\mathbf{u}}_{i,j}(t)\bar{L}_{i,j}(x) \tag{4}$$

where the SV basis functions $\bar{L}_{i,j}(x)$ are defined by

$$\frac{1}{x^{\mathrm{b}}_{i,j+\frac{1}{2}} - x^{\mathrm{b}}_{i,j-\frac{1}{2}}} \int_{x^{\mathrm{b}}_{i,j-\frac{1}{2}}}^{x^{\mathrm{b}}_{i,j+\frac{1}{2}}} \bar{L}_{i,k}(x)\mathrm{d}x = \delta_{jk} \tag{5}$$

with $\delta_{jk}$ the Kronecker delta function. Using this solution polynomial, the fluxes at the CV-boundaries can be approximated and the right-hand-side of (2) can be evaluated. At the interface between two cells, a Riemann solver $\tilde{\mathbf{F}}^{\mathrm{R,SV}}(\mathbf{u}_{\mathrm{L}}, \mathbf{u}_{\mathrm{R}})$ is used to deal with the discontinuity in the numerical solution. Eq. (2) is then written as

$$\frac{\mathrm{d}\bar{\mathbf{u}}_{i,j}}{\mathrm{d}t} = -\frac{\mathbf{F}^{\mathrm{SV}}_{i,j+\frac{1}{2}} - \mathbf{F}^{\mathrm{SV}}_{i,j-\frac{1}{2}}}{x^{\mathrm{b}}_{i,j+\frac{1}{2}} - x^{\mathrm{b}}_{i,j-\frac{1}{2}}} \tag{6}$$

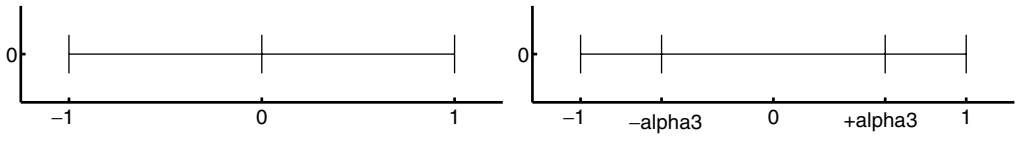


Fig. 1. Second- (left) and third-order (right) accurate 1D SV cells, plotted in a coordinate system local to the cell ($-1 \leqslant \xi \leqslant +1$).